Anatomical Science International (2019) 94:163–171
https://doi.org/10.1007/s12565-018-0462-x

ORIGINAL ARTICLE

Nisin, a food preservative produced by *Lactococcus lactis*, affects the localization pattern of intermediate filament protein in HaCaT cells

Norio Kitagawa[1] · **Takahito Otani**[1] · **Tetsuichiro Inai**[1]

Received: 17 May 2017 / Accepted: 12 October 2018 / Published online: 23 October 2018

Abstract

Nisin is a food preservative produced by *Lactococcus lactis* subsp. *lactis*. Previous blood biochemical research revealed that nisin has physiological effects in mammals; although the site of action has yet to be identified, keratinocytes have been proposed as a possible target. In this study, we investigated whether nisin affects keratinocytes by examining the effects on eukaryotic intermediate filaments in HaCaT human keratinocytes. Treatment with 93 μg/ml nisin for 24 h decreased the localization of the intermediate filament proteins cytokeratin (CK)5 and CK17 at the cell periphery, which were distributed in a limited area in a ring- or net-like shape. However, this was not observed upon treatment for 6 h. The results of a serial dilution assay revealed that the effect on CK17 localization depends on the nisin concentration and were observed at ≥47 μg/ml. Moreover, this effect was partially blocked by treatment with the calcium channel blocker bepridil. Thus, despite the long history of nisin as being safe for humans, it has measurable effects on the keratinocyte cytoskeleton. Our findings also indicate that CK5 and CK17 can serve as markers for evaluating the effects of nisin on keratinocytes.

Keywords Cytokeratin 17 · Cytokeratin 5 · HaCaT · Keratinocyte · Nisin

Introduction

Bacteriocins are antimicrobial peptides produced by various bacteria. Nisin is a type of bacteriocin produced by some strains of *Lactococcus lactis* subsp. *lactis*. Although many bacteriocins are only effective against specific bacteria groups, nisin has broad-spectrum effects (Brotz and Sahl 2000; Bonev et al. 2000). Due to its heat stability and tolerance of low pH, nisin is widely used as a food preservative (Delves-Broughton et al. 1996; Cleveland et al. 2001; CFSAN/Office of Food Additive Safety 2016). Nisin is a polycyclic antibacterial peptide comprising 34 amino acid residues, with an overall positive charge and amphipathic properties; it disrupts the integrity of the cell membrane by forming short-lived pores (Moll et al. 1997; Brotz et al. 1998), leading to rapid efflux of cellular materials (e.g., amino acids and adenosine triphosphate) from bacteria and thereby disrupting the cell (Gao et al. 1999). The US Food and Drug Administration reported that nisin is "generally recognized as safe" for use as a preservative in human foods (Federal Register: 53 FR 11247, April 6, 1988); there were no obvious effects observed for concentrations <83.25 mg/kg in humans and <66.7 mg/kg in mouse. One gram of food in the USA and other countries contains about 250 μg nisin (Cleveland et al. 2001); 0.1–300 μg/ml nisin is contained in mouthwashes (Bartlett et al. 1998), whereas 300–400 μg/ml has a contraceptive effect in humans (Aranha et al. 2004).

Nisin has not been found to affect normal epithelial tissue (Reddy et al. 2004; Joo et al. 2012; Maher and McClean 2006); however, a blood biochemical study revealed a dose-dependent decrease in total cholesterol and phospholipid levels in rats treated with nisin, although the physiological basis for this effect is unclear (Food Safety Commission Japan, 00108, January 31, 2008). More recently, nisin was found to induce apoptosis in cancer-derived cells, although

Electronic supplementary material The online version of this article (https://doi.org/10.1007/s12565-018-0462-x) contains supplementary material, which is available to authorized users.

✉ Norio Kitagawa
kitagawa@college.fdcnet.ac.jp

Takahito Otani
otani@college.fdcnet.ac.jp

Tetsuichiro Inai
tinaitj@college.fdcnet.ac.jp

[1] Department of Morphological Biology, Fukuoka Dental College, 2-15-1 Tamura, Sawara-ku, Fukuoka 814-0193, Japan

its effects on normal epithelia have still not been found (Joo et al. 2012).

Keratinocytes are the main cells of the stratified squamous epithelium that lines the surface of the oral cavity and esophagus (Ross and Pawlina 2015). Keratinocytes are exposed to nisin present in ingested foods before its digestion by proteases. Intermediate filaments are a major cytoskeletal component that form a cytoplasmic network encircling the nucleus and extending to the plasma membrane (Ross and Pawlina 2015). We speculated that nisin acts on keratinocytes prior to its digestion by proteases.

To test this hypothesis, we evaluated the effects of nisin on keratinocytes by examining the

changes in the distribution of eukaryotic intermediate filament proteins, namely CK5 and CK17, in HaCaT cells, which is a widely used immortal human keratinocyte cell line that has uniform epithelial architecture when transplanted into nude mice (Boukamp et al. 1988). Therefore, HaCaT cells are considered as a good model for the stratified squamous epithelium, which is mostly composed of keratinocytes (Wu et al. 2012). Eukaryote- and prokaryote-type intermediate filaments differ in terms of their protein components (Ausmees et al. 2003; Esue et al. 2010); the former include cytokeratin CK5 and CK17, which are expressed in cultured HaCaT cells (Kitagawa et al. 2014). Changes in CK distribution are correlated with cell growth and epithelialization, cell migration, and cytoarchitecture (Paladini et al. 1996; Foisner 1997). Due to their ubiquitous distribution in the cytoplasm, intermediate filament proteins can be used for detection of previously undetected alterations brought about by nisin.

Materials and methods

Materials

Food-grade nisin was obtained from Sigma–Aldrich (St. Louis, MO, USA). Bepridil was purchased from Enzo Life Sciences (Farmingdale, NY, USA). Fetal bovine serum (FBS) was from Biowest (Santiago, Chile). The ten-well glass slides printed with highly water-repellent marks (6 mm in diameter) were from Matsunami Glass Industry (Osaka, Japan; cat. no. TF1006).

Cell culture and treatment

HaCaT cells (Boukamp et al. 1988) were cultured in Dulbecco's modified Eagle's medium (DMEM) supplemented with 10 % FBS, 2 mM glutamine, 100 µg/ml streptomycin, and 100 mg/ml penicillin. This growth medium contained approximately 2.2 mM calcium. Cells were seeded at a subconfluent density (1.2×10^5 cells/cm^2) in ten-well glass slides; the medium was changed the following day, and the cells were cultured for 2 days. After culturing for 2 days, cells were treated for 24 h with 23, 47, 93, or 186 µg/ml nisin in growth medium. Nisin was diluted in 0.05 % acetic acid before addition to the medium. As control, cells were grown for 24 h in medium containing 0.0015 % acetic acid or 0.0015 % acetic acid plus 0.01 % dimethylsulfoxide (DMSO).

The calcium channel blocker bepridil was dissolved in DMSO to 50 mM to form a stock solution (Wang et al. 1999; Zhang et al. 2014). After 2 days of culture, cells were treated for 24 h with either 5 µM bepridil and 93 µg/ml nisin (nisin-bepridil) or 5 µM bepridil alone (bepridil) in growth medium to evaluate the effects of both agents.

Recovery assay

To assess the reversibility of the effects of nisin, cells were treated with growth medium containing 93 µg/ml nisin for 24 h, washed once with DMEM, and further incubated in growth medium without (recovery) or with 93 µg/ml nisin (2-day nisin treatment) for 24 h.

Immunofluorescence microscopy

Cells were fixed with 1 % paraformaldehyde in phosphate-buffered saline (PBS) for 10 min, rinsed with PBS, and permeabilized in 0.2 % Triton-X 100 in PBS for 15 min. The cells were then rinsed with PBS and incubated in PBS containing 1 % bovine serum albumin (BSA-PBS) for 15 min to block nonspecific binding. They were then incubated with primary antibodies at room temperature for 1 h.

After washing four times with PBS, the cells were incubated with appropriate secondary antibodies diluted 1:400 in BSA-PBS for 30 min at room temperature in the dark. The cells were then rinsed four times with PBS and mounted in VECTASHIELD containing the nuclear counterstain 4′,6-diamidino-2-phenylindole (Vector Laboratories, Burlingame, CA, USA). Images were obtained using an LSM710 confocal laser scanning microscope (Zeiss, Oberkochen, Germany) with a 20×/0.75 NA objective or 63×/1.4 NA or 100×/1.4 NA oil objectives. *Z*-stacks were obtained at constant *Z* interval. Images and montages were generated using Zeiss Zen software and Adobe Photoshop (Adobe Systems, San Jose, CA, USA). The antibodies used were as follows: Rabbit polyclonal anti-CK5 (cat. no. SAB4501651, 1:100) and anti-CK17 (cat. no. SAB4501662, 1:100) antibodies were obtained from Sigma–Aldrich; Mouse monoclonal anti-desmoglein (DSG)3 antibody (cat. no. GTX76040, 1:100) was from GeneTex (Irvine, CA, USA); mouse monoclonal anti-β-catenin antibody (cat. no. C19220, 1:100) was from BD Transduction Laboratories (Lexington, KY, USA); Anti-mouse and -rabbit IgG conjugated with either Alexa

488 (cat. nos. A11008 and A11034) or Alexa 568 (cat. nos. A11031 and A11036) (all from Molecular Probes, Eugene, OR, USA) were used as secondary antibodies.

Image analysis

Images (512 × 512 pixels) including those of control cells labeled for CK17 were acquired in four separate experiments using a confocal microscope. Images of nisin-treated cells were obtained using optimized conditions. Three indices, i.e., CK17 localization area in a single image (localization index), CK17 localization area in a *Z*-stack (localization index), and CK17 ring-like localization in a *Z*-stack (ring index), were calculated using ImageJ software (http://rsb.info.nih.gov/ij).

Image projections were generated from *Z*-stacks. Cell numbers were counted using the "Analyze particles" command of ImageJ (Li et al. 2011). The analysis was carried out after confirming that there was no difference between the number of cells and number of slices in *Z*-stacks. Pixels with values $150 \leq x \leq 220$ were counted as CK17 positive for the CK17 localization area index of a single image, while those with values $150 \leq x \leq 254$ were counted as CK17 positive for the CK17 localization area index of *Z*-stacks. The CK17-positive pixel range was defined based on exclusion of pixels where CK17 was not localized. The upper limit of the CK17-positive pixel range was defined as not containing non-CK17 labeling, including intrinsic fluorescence from dead cells. Pixels with values ≤ 20 were counted as CK17 negative in both single images and *Z*-stacks. The pixel range was determined so as to exclude those containing CK17. Both localization indices are expressed as the value obtained by dividing the number of CK17-positive pixels by the number of CK17-negative pixels in each image.

Ring-like localization was quantified using the "Cell counter" command in ImageJ. We defined ring-like localization as strong, ring-shaped labeling; weak immunoreactivity, such as that observed in tricellular contacts, was not counted. We considered only ring-like localization with diameter >2 μm. The ring index was expressed as the total number of instances of ring-like CK17 localization in each image (512 × 512 pixels).

TUNEL assay

Apoptotic cells were detected by terminal deoxynucleotidyl transferase-mediated dUTP nick-end labeling assay (TUNEL) using an in situ apoptosis detection kit (Takara Bio, Otsu, Japan) according to the manufacturer's protocol, with a few modifications. Briefly, cells were seeded and grown for 24 h in medium containing 93 μg/ml nisin or 0.0015% acetic acid as described above. After washing with PBS, positive control cells were exposed to ultraviolet light for 30 min before fixation in 4% paraformaldehyde in PBS for 30 min. After washing with PBS, the cells were treated with permeabilization solution on ice and were again washed with PBS before incubation with fluorescein-labeled dUTP and TdT enzyme at 37 °C for 60 min in a wet box in the dark.

Viability assay

HaCaT cell viability was determined based on quantification of adenosine triphosphate (ATP) levels using the Cell Titer-Glo 2.0 Assay kit (Promega, Madison, WI, USA), which detects the presence of metabolically active cells. Briefly, cells were seeded in a 96-well plate at subconfluent density (1.2×10^5 cells/cm^2); the medium was changed the next day, and cells were cultured for 2 days. On the third day, 93 μg/ml nisin was added to the cells. After incubation for 24 h, Cell Titer-Glo reagent was added, and luminescence was measured with a Multilabel reader (PerkinElmer, Santa Clara, CA, USA).

Calcium measurements

Changes in intracellular calcium concentration caused by bepridil were measured with the fluorescent dye Fluo-4 AM (Thermo Fisher Scientific) according to the manufacturer's protocol. As a control, cells were grown in medium containing 0.0015% acetic acid plus 0.01% DMSO. HaCaT cells were incubated with Fluo-4 AM for 30 min at 37 °C and then maintained for 30 min at room temperature. Fluorescence emission was measured using a Multilabel reader (PerkinElmer) at Ex 485 nm/Em 535 nm.

Statistical analysis

Values are expressed as mean ± standard error (SE). Differences between groups were evaluated with the unpaired *t* test with Welch's correction, except for the results of the viability assay, for which the Mann–Whitney *U* test was used. $P < 0.05$ was considered significant.

Results

Nisin induces ring-like localization of CK5 and CK17

CK17 immunoreactivity was observed throughout the cytoplasm of untreated control cells (Fig. 1A-a, bright-green cytoplasm in Fig. 1B-a); in particular, CK17 immunoreactivity observed at the periphery of cells was similar to or stronger than that observed in the other parts of cytoplasm (Fig. 1A-a). At the cell periphery, CK17 was distributed in a line perpendicular to the cell surface (Fig. 1A-a, B-a, Supplementary Fig. 1A-a).

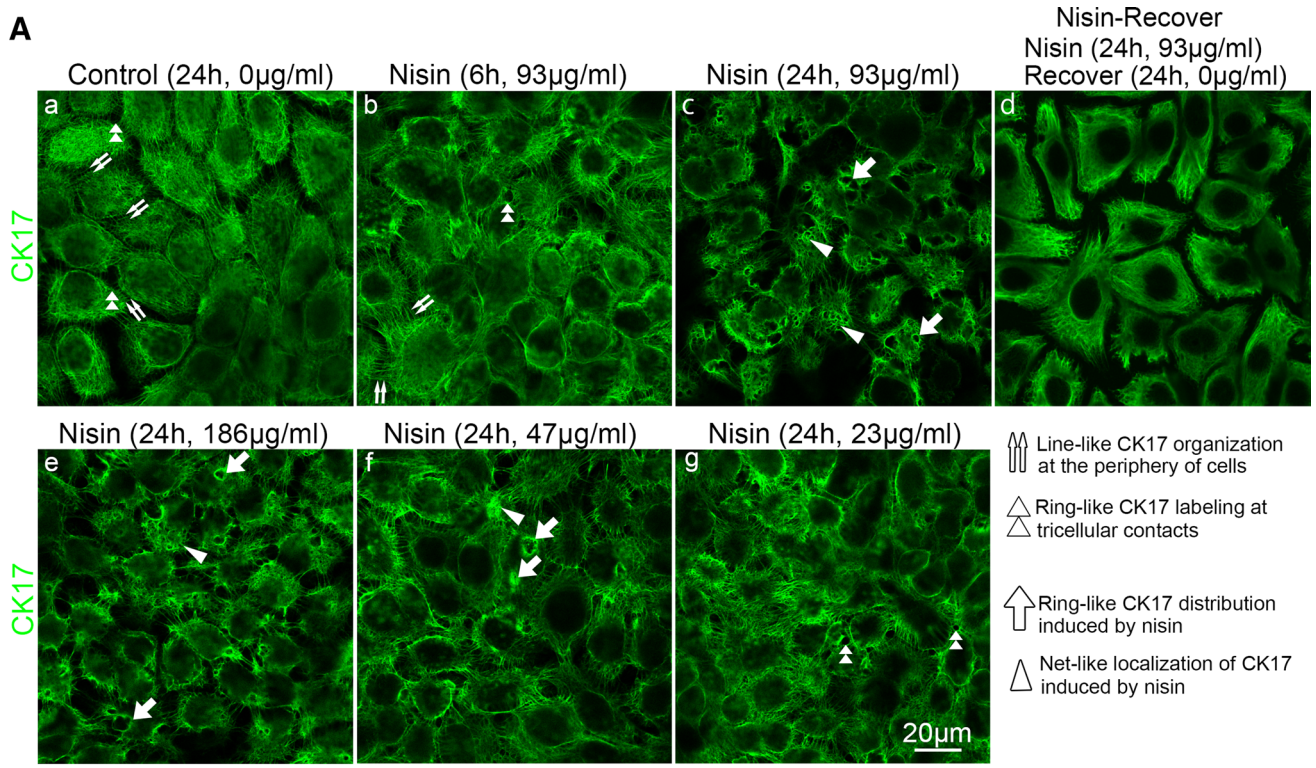
A
Control (24h, 0μg/ml)
Nisin (6h, 93μg/ml)
Nisin (24h, 93μg/ml)
Nisin-Recover
Nisin (24h, 93μg/ml)
Recover (24h, 0μg/ml)
CK17
a
b
c
d
Nisin (24h, 186μg/ml)
Nisin (24h, 47μg/ml)
Nisin (24h, 23μg/ml)
e
f
g
20μm
Line-like CK17 organization at the periphery of cells
Ring-like CK17 labeling at tricellular contacts
Ring-like CK17 distribution induced by nisin
Net-like localization of CK17 induced by nisin

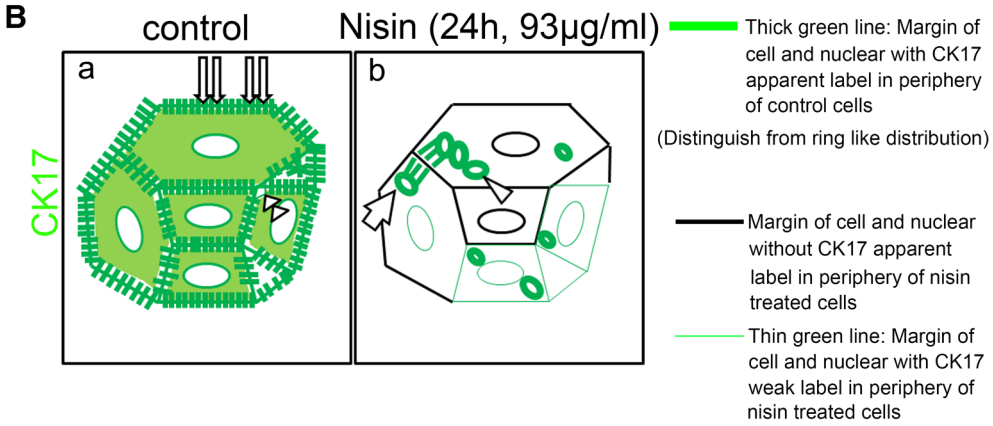
B
control
Nisin (24h, 93μg/ml)
CK17
a
b
Thick green line: Margin of cell and nuclear with CK17 apparent label in periphery of control cells
(Distinguish from ring like distribution)
Margin of cell and nuclear without CK17 apparent label in periphery of nisin treated cells
Thin green line: Margin of cell and nuclear with CK17 weak label in periphery of nisin treated cells

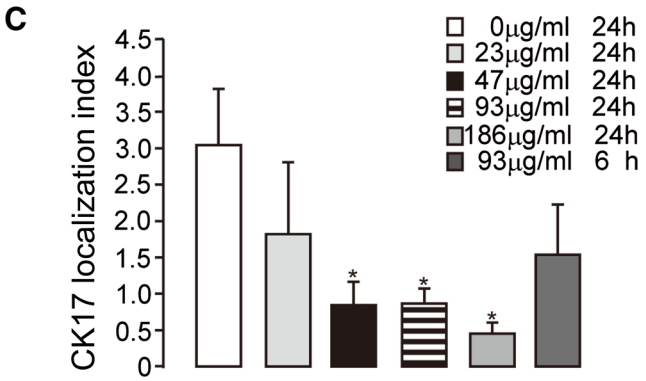
C
CK17 localization index
4.5
4.0
3.5
3.0
2.5
2.0
1.5
1.0
0.5
0
0μg/ml 24h
23μg/ml 24h
47μg/ml 24h
93μg/ml 24h
186μg/ml 24h
93μg/ml 6 h
*
*
*

◂**Fig. 1** Nisin prevents CK17 localization at the cell periphery and induces CK17 ring-like distribution in the cytoplasm of HaCaT cells. **A** and **B** HaCaT cells were treated for 6 h and 24 h with the indicated concentrations of nisin. After nisin treatment, cells for recovery assay were followed by 24 h culture in nisin-free medium (Nisin-Recover). Immunohistochemical analysis of CK17 (green fluorescence) was performed. Panel B shows a schematic illustration of the CK17 distribution upon treatment with nisin for 24 h. The meaning of each indicator is illustrated. **C** CK17 localization index in cells treated with 93 μg/ml nisin for 6 and 24 h and dilution series of nisin. Values expressed as mean ± SE ($n > 15$ in four independent experiments). *$P < 0.05$ versus control. Scale bars in A represent 20 μm

Treatment with 93 μg/ml nisin for 24 h decreased the peripheral distribution of CK17 (Fig. 1A-c, B-b, Supplementary Fig. 1A-b). The accumulated CK17 protein aligned along cell membrane and nuclear membrane was less apparent or almost undetectable when treated with nisin (Fig. 1A-c, B-b). The CK17 line perpendicular to the cell surface was less apparent in cells treated with nisin (Fig. 1A-c, B-b). Ring-like distribution patterns of CK17 around tricellular contacts in control cells were increased by 93 μg/ml nisin treatment. Additionally, 93 μg/ml nisin also induced ring-like distribution in areas other than tricellular contacts (thick arrow in Fig. 1A-c, B-b and Supplementary Fig. 1A-b), resulting in a net-like distribution in the cytoplasm formed by small, ring-like aggregates (arrowhead in Fig. 1A-c, B-b and Supplementary Fig. 1A-b); however, this was not observed in cells treated for 6 h with nisin (Fig. 1A-b). Removal of nisin and subsequent cell culture for 24 h in nisin-free medium restored the peripheral distribution of CK17 (Fig. 1A-d).

Serial dilution experiments revealed that this change in CK17 distribution was dependent on nisin concentration; whereas some CK17 was observed at the cell periphery with 47 μg/ml nisin treatment, 186 μg/ml or 93 μg/ml nisin treatment drastically altered these distribution patterns (Fig. 1A-c, e, f). Although the CK17 distribution at nisin concentration of 23 μg/ml was almost the same as that of controls, the CK17 ring-like structures showed significant increase in their number in a nisin-dose-dependent manner (Fig. 1A-c, e–g). We determined the CK17 localization index, which indicates the number of pixels in the CK17-positive areas. Nisin treatment (24 h) decreased the index ($P < 0.05$; Fig. 1C) in a concentration-dependent manner. A significant difference was observed for cells treated with nisin concentrations over 47 μg/ml for 24 h.

Z-stack images showed CK17 ring-like distribution patterns observed in the cytoplasm (Supplementary Fig. 1B). Strong CK17 immunoreactivity extended in various directions in nisin-treated cells (Supplementary Fig. 1A-b). The ring index was higher in nisin-treated cells than in control cells (9.27 ± 1.17 versus 0.67 ± 0.17, $P < 0.05$; Supplementary Fig. 1C). The CK17 localization index (*Z*-stack) revealed a decreased number of CK17-positive pixels in nisin-treated cells. The number of pixels corresponding to CK17 distributed in a line at the cell periphery in control cells was greater than that of CK17 localized in a ring or net in nisin-treated cells (0.84 ± 0.19 versus 0.33 ± 0.05; $P < 0.05$; Supplementary Fig. 1C).

CK5, another intermediate filament protein, exhibited the similar localization pattern as CK17 in control cells, cells treat with nisin for 6 h, and cells treated with nisin for 24 h (Fig. 2a–c). Serial dilution experiments revealed that this change in CK5 localization was also dependent on the nisin concentration (Fig. 2c, g–i).

The nisin-induced decrease in peripheral CK17 localization was partially reversed in the presence of the calcium channel blocker bepridil (Fig. 3a, Supplementary Fig. 1A-c). In addition, treatment with both nisin and bepridil increased the immunoreactivity of CK17 and changed its distribution form from surrounding the nucleus to the plasma membrane (Supplementary Fig. 1A-c); bepridil alone induced a similar distribution as in control cells (Fig. 3b, Supplementary Fig. 1A-d). Bepridil blocked calcium influx in both control and nisin-treated cells (Supplementary Fig. 2). There was no apparent increase in apoptosis after 24 h of treatment with 93 μg/ml nisin relative to untreated control cells (Supplemental Fig. 3A). However, cell viability was slightly decreased (95.4 ± 1.3 nisin-treated cells versus 100.0 ± 2.0 in control cells, $n = 14$; $P < 0.05$, Mann–Whitney *U* test) (Supplementary Fig. 3B).

Nisin acts on a desmosomal protein that anchors intermediate filaments

DSG3 is a desmosomal protein that anchors intermediate filaments to sites of intercellular contact. DSG3 and CK17 were frequently colocalized in control cells (Fig. 4A), and DSG3 was observed at intercellular contacts (Fig. 4A, B-a). However, this localization of DSG3 was abolished by nisin treatment (Fig. 4B-b), which was not reversed by bepridil (Fig. 4B-c). Bepridil alone increased DSG3 accumulation at intercellular contacts relative to control cells (Fig. 4B-d).

Nisin affects junctional proteins that do not anchor intermediate filaments

β-Catenin, a major component of adherens junctions, was specifically localized at the periphery of control cells (Fig. 4C). This was decreased in nisin-treated cells, resulting in diffuse β-catenin localization in the cytoplasm, and this effect was partially blocked by bepridil, although diffuse β-catenin localization was not blocked by bepridil in certain nisin-treated cells. Bepridil treatment alone did not decrease the diffuse β-catenin immunoreactivity in the cytoplasm.

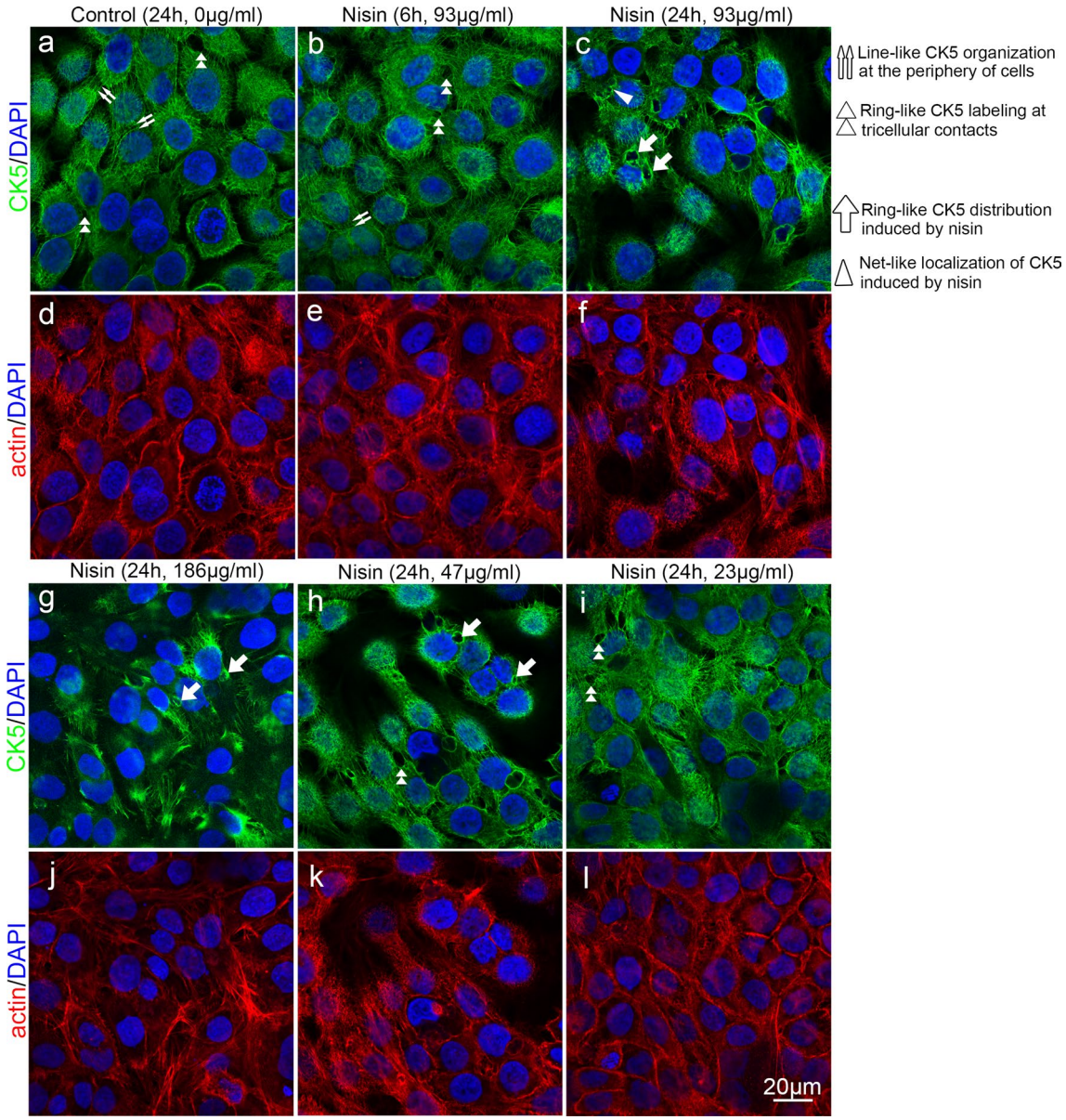

Fig. 2 Nisin prevents CK5 localization at the cell periphery and induces a ring-like CK5 distribution in the cytoplasm of HaCaT cells. HaCaT cells were treated for 6 or 24 h with the indicated concentrations of nisin. Immunohistochemical analysis of CK5 (green fluorescence) and actin (red fluorescence) was performed. The meaning of each indicator is illustrated. Scale bars in (l) represent 20 μm

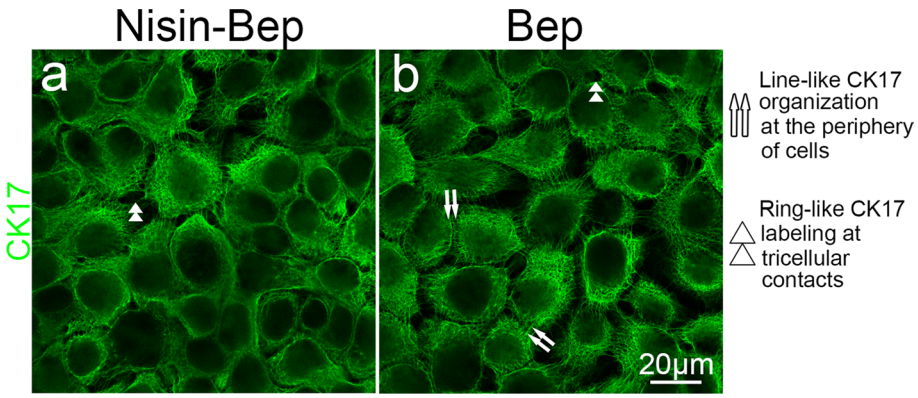

Fig. 3 Bepridil partially blocked perturbation by nisin. Cells were treated with either 5 μM bepridil (Bep) alone or 93 μg/ml nisin and 5 μM bepridil (Nisin + Bep) for 24 h. Immunohistochemical analysis of CK17 (green fluorescence) was performed. The meaning of each indicator is illustrated. Scale bar in (b) represents 20 μm

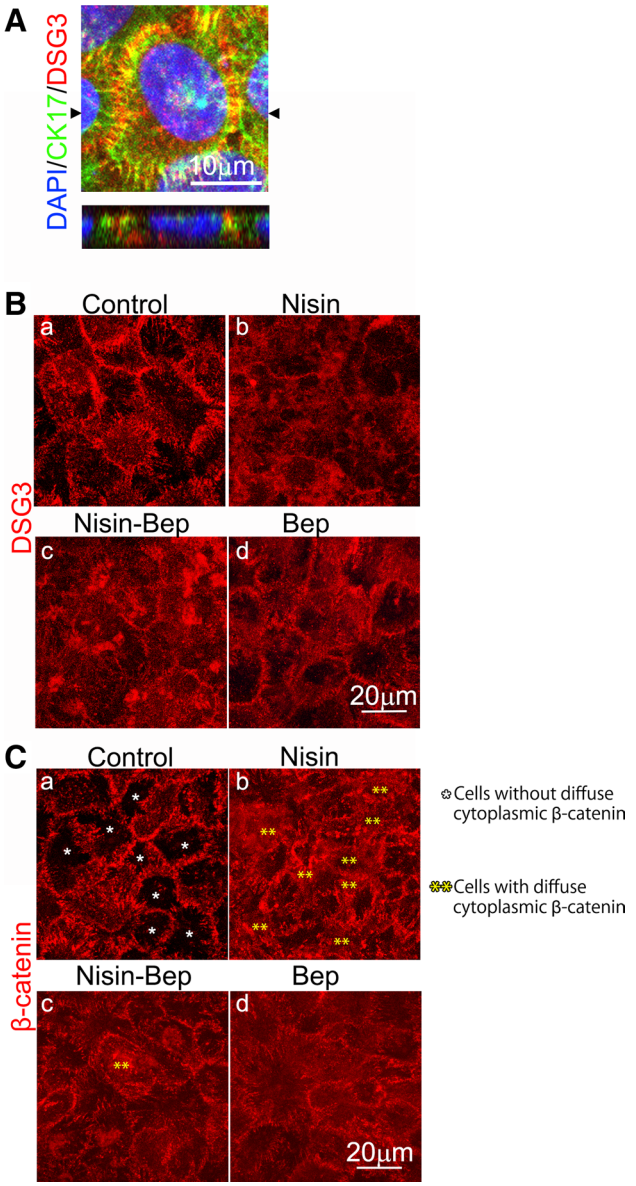

Fig. 4 Nisin treatment alters the localization of DSG3 and β-catenin. **A** Immunofluorescence images of CK17 (green fluorescence) and DSG3 (red fluorescence) in cells treated with growth medium containing vehicle. CK17 and DSG3 colocalized at the cell periphery. Black arrowhead indicates the position selected for *XZ* section analysis. **B**, **C** Immunofluorescence images of DSG3 and β-catenin treated without nisin (control), 93 μg/ml nisin, 93 μg/ml nisin and 5 μM bepridil (nisin + Bep), or 5 μM bepridil (Bep) for 24 h. The meaning of each indicator is illustrated. **A**–**C** *Z*-stack projections. Scale bars in A and B, C represent 10 and 20 μm, respectively

Discussion

We found that nisin has observable effects in eukaryotic cells. We demonstrated that nisin treatment altered the intermediate filament distribution in keratinocytes. Within cells derived from normal epithelium, CK5 and CK17 in keratinocytes are the only cellular components shown to be altered by nisin treatment, and their distribution changes were observed in this work. Due to their ubiquitous distribution in the cytoplasm, CK5 and CK17 intermediate filaments are useful markers for investigating morphological changes caused by nisin. Since CK5 and CK17 show similar distribution patterns, both can serve as cytological indicators for determination of the effect of nisin under these experimental conditions.

The calcium channel blocker bepridil blocked calcium influx (Supplementary Fig. 2). Bepridil also partially blocked the nisin-induced changes (Fig. 3a). Our results suggest that calcium influx should be focused on when analyzing the effects of nisin in keratinocytes. Studies that have demonstrated the effects of nisin against keratinocytes (including ours as well as a previous study using cancer cells) used DMEM supplemented with 10 % FBS and calcium for cultures (Fin. approximately 2.2 mM calcium); future studies should therefore examine the effects of nisin in various cell lines under these culture conditions (Joo et al. 2012).

Previous studies using normal vaginal epithelium or cells derived from normal keratinocytes did not report abnormalities (Joo et al. 2012; Aranha et al. 2004); however, those authors did not investigate intermediate filament proteins, and the analytical methods were limited to microscopic examination of edematous thickening or simple viability tests. Therefore, their findings do not contradict those reported herein.

Nisin alters the organization of the plasma membrane lipid bilayer (Scherer et al. 2015; Hsu et al. 2004; Wiedemann et al. 2004). We hypothesized that the impairment of the CK5 and CK17 distribution is related to disruption of the lipid bilayer indirectly. DSG3 is a component of the desmosome that anchors intermediate filaments to the lipid bilayer. In contrast, β-catenin is a component of adherens junctions that does not anchor intermediate filaments, but directly binds to lipid bilayer. The observed changes in the localization of both proteins might indicate nisin-induced lipid bilayer disorganization, a recently reported phenomenon (Scherer et al. 2015; Hsu et al. 2004; Wiedemann et al. 2004). Our hypothesis is well consistent with this mechanism.

We inferred from *Z*-stack images that this ring-like distribution is likely to be an intracellular network rather than a structure that extends to several cells (Supplemental Fig. 1B). It is therefore possible that the ring-like distribution represents changes caused by closed membrane structure, like vacuole. Several diseases are known to cause intracellular vacuoles in keratinocytes, although the mechanism has not been revealed (Lacz et al. 2005; Eskin-Schwartz et al. 2017). Therefore, it is not surprising that nisin causes vacuoles in keratinocytes. Based on the

results of this study, it can be suggested that the presence of vacuoles influences the distributions of CK5 and CK17. However, there is another hypothesis. As some proliferating HaCaT cells were released from the cell monolayer under control conditions, we speculate that disturbance of the cell membrane and intracellular junctions by nisin caused these ring-like distribution patterns in released cells and those in their immediate surroundings. Consistent with this notion, changes in distribution induced by nisin were observed after 24 h, which is similar to the doubling time (Seo et al. 2015) (Fig. 1A-b, c, 2b, c).

The effects of nisin were no longer observed at 23 µg/ml (Fig. 1A-g), which is the concentration in about one-tenth of foods and other products containing high concentrations of nisin (250 µg nisin per gram of food) (Cleveland et al. 2001). Thus, based on our data, nisin diluted in saliva cannot be effective since the concentration is much lower than the effective concentration demonstrated in our work. Nonetheless, it is possible that nisin has significant effects against keratinocytes in patients who have trouble with dilution, such as those with xerostomia. After investigating whether nisin acts on the epithelium under physiological conditions, it will be important to investigate retention and enrichment effects in the oral cavity.

Nisin has recently been recognized and evaluated as a potential anticancer agent, preservative, and active ingredient in mouthwash (Joo et al. 2012; Reddy et al. 2004; Bartlett et al. 1998). Given our findings that nisin affects the cytoskeleton of keratinocytes derived from normal epithelium, it is important to evaluate the degree to which these effects can be generalized to epithelial tissue. Additional studies are also needed to clarify the relationship between the effects of nisin observed here and the increased blood cholesterol concentrations in rat reported recently (Food Safety Commission Japan, 00108, January 31, 2008), which may arise from cell membrane damage.

In summary, the change in the CK5 and CK17 distribution in keratinocytes, under the current culture conditions, is the only observable alteration shown to be caused by nisin treatment. Therefore, CK5 and CK17 are important cytological indicators in the investigation of morphological changes caused by nisin. We showed decreased peripheral distribution and increased ring-like distribution of CK5 and CK17 when treated with nisin. These effects correlated with the concentration and duration of nisin treatment. Based on our results, lipid bilayer disruption and intracellular vacuole formation are hypothesized to be related to the change in distribution of CK5 and CK17.

Funding This study was funded by a Japan Society for the Promotion of Science KAKENHI grant (grant nos. 15K21564, 17K18302) and Regenerative Medicine Center public research funding (2013) from Fukuoka Dental College.

Compliance with ethical standards

Conflict of interest The authors declare that they have no conflicts of interest.

References

Aranha C, Gupta S, Reddy K (2004) Contraceptive efficacy of antimicrobial peptide nisin: in vitro and in vivo studies. Contraception 69:333–338

Ausmees N, Kuhn JR, Jacobs-Wagner C (2003) The bacterial cytoskeleton: an intermediate filament-like function in cell shape. Cell 115:705–713

Bartlett M, Mcconville PS, Price F (1998) Compositions containing nisin. Google patents

Bonev BB, Chan WC, Bycroft BW, Roberts GC, Watts A (2000) Interaction of the lantibiotic nisin with mixed lipid bilayers: a ^{31}P and ^{2}H NMR study. Biochemistry 39:11425–11433

Boukamp P, Petrussevska RT, Breitkreutz D, Hornung J, Markham A, Fusenig NE (1988) Normal keratinization in a spontaneously immortalized aneuploid human keratinocyte cell line. J Cell Biol 106:761–771

Brotz H, Sahl HG (2000) New insights into the mechanism of action of lantibiotics–diverse biological effects by binding to the same molecular target. J Antimicrob Chemother 46:1–6

Brotz H, Josten M, Wiedemann I et al (1998) Role of lipid-bound peptidoglycan precursors in the formation of pores by nisin, epidermin and other lantibiotics. Mol Microbiol 30:317–327

CFSAN/Office of Food Additive Safety (2016) Agency response letter GRAS notice no. GRN 000065. http://www.fda.gov/food/ingredientspackaginglabeling/gras/noticeinventory/ucm153977.htm. Accessed 20 Dec 2000

Cleveland J, Montville TJ, Nes IF, Chikindas ML (2001) Bacteriocins: safe, natural antimicrobials for food preservation. Int J Food Microbiol 71:1–20

Delves-Broughton J, Blackburn P, Evans RJ, Hugenholtz J (1996) Applications of the bacteriocin, nisin. Antonie Van Leeuwenhoek 69:193–202

Eskin-Schwartz M, Drozhdina M, Sarig O et al (2017) Epidermolytic ichthyosis sine epidermolysis. Am J Dermatopathol 39:440–444

Esue O, Rupprecht L, Sx Sun, Wirtz D (2010) Dynamics of the bacterial intermediate filament crescentin in vitro and in vivo. PLoS One 5:e8855

Foisner R (1997) Dynamic organisation of intermediate filaments and associated proteins during the cell cycle. BioEssays 19:297–305

Gao Y, Van Belkum MJ, Me Stiles (1999) The outer membrane of gram-negative bacteria inhibits antibacterial activity of brochocinc. Appl Environ Microbiol 65:4329–4333

Hsu ST, Breukink E, Tischenko E et al (2004) The nisin-lipid II complex reveals a pyrophosphate cage that provides a blueprint for novel antibiotics. Nat Struct Mol Biol 11:963–967

Joo NE, Ritchie K, Kamarajan P, Miao D, Yl Kapila (2012) Nisin, an apoptogenic bacteriocin and food preservative, attenuates HNSCC tumorigenesis via CHAC1. Cancer Med 1:295–305

Kitagawa N, Inai Y, Higuchi Y, Iida H, Inai T (2014) Inhibition of JNK in HaCat cells induced tight junction formation with decreased expression of cytokeratin 5, cytokeratin 17 and desmoglein 3. Histochem Cell Biol 142:389–399

Lacz NL, Schwartz RA, Kihiczak G (2005) Epidermolytic hyperkeratosis: a keratin 1 or 10 mutational event. Int J Dermatol 44:1–6

Li S, Nv Guz, Sokolov I (2011) A modified in vitro stripping method to automate the calculation of geometry of corneocytes imaged with fluorescent microscopy: example of moisturizer treatment. Skin Res Technol 17:213–219

Maher S, Mcclean S (2006) Investigation of the cytotoxicity of eukaryotic and prokaryotic antimicrobial peptides in intestinal epithelial cells in vitro. Biochem Pharmacol 71:1289–1298

Moll GN, Clark J, Chan WC et al (1997) Role of transmembrane pH gradient and membrane binding in nisin pore formation. J Bacteriol 179:135–140

Paladini RD, Takahashi K, Bravo NS, Coulombe PA (1996) Onset of re-epithelialization after skin injury correlates with a reorganization of keratin filaments in wound edge keratinocytes: defining a potential role for keratin 16. J Cell Biol 132:381–397

Reddy KV, Aranha C, Gupta SM, Yedery RD (2004) Evaluation of antimicrobial peptide nisin as a safe vaginal contraceptive agent in rabbits: in vitro and in vivo studies. Reproduction 128:117–126

Ross MH, Pawlina W (2015) Histology: a text and atlas. Wolters Kluwer Health, Philadelphia

Scherer KM, Spille JH, Sahl HG, Grein F, Kubitscheck U (2015) The lantibiotic nisin induces lipid ii aggregation, causing membrane instability and vesicle budding. Biophys J 108:1114–1124

Seo GY, Ho MT, Bui NT et al (2015) Novel naphthochalcone derivative accelerate dermal wound healing through induction of epithelial-mesenchymal transition of keratinocyte. J Biomed Sci 22:47

Wiedemann I, Benz R, Sahl HG (2004) Lipid II-mediated pore formation by the peptide antibiotic nisin: a black lipid membrane study. J Bacteriol 186:3259–3261

Wang JC, Kiyosue T, Kiriyama K, Arita M (1999) Bepridil differentially inhibits two delayed rectifier K(+) currents, I(Kr) and I(Ks), in guinea-pig ventricular myocytes. Br J Pharmacol 128:1733–1738

Wu X, Chen P, Sonis ST, Lingen MW, Berger A, Toback FG (2012) A novel peptide to treat oral mucositis blocks endothelial and epithelial cell apoptosis. Int J Radiat Oncol Biol Phys 83:e409–e415

Zhang CX, Cui W, Zhang M et al (2014) Role of Na^+/Ca^{2+} exchanger (NCX) in modulating postovulatory aging of mouse and rat oocytes. PLoS One 9:e93446